2026 JULY 19–22 VANCOUVER, BC
JOINT AAPM | COMP MEETING

# A library of experimentally derived microscale blood and lymphatic vasculature models for applications to radiopharmaceutical dosimetry

Julia D. Withrow[1], Iulia Maria Berianu[1], Luna Trujillo-Suarez[1], Nien-Wen Hu[1], Mir Md Nasim Hossain[2], Wyatt W. Smither[1], Lazaro L. Fuentes Alfonso[1], Ryan Q. Walker[1], Peter Balogh[2], Walter L. Murfee[1], and Wesley E. Bolch[1]

[1]J. Crayton Pruitt Family Department of Biomedical Engineering, University of Florida [2]Department of Mechanical and Industrial Engineering, New Jersey Institute of Technology

## INTRODUCTION

In radiopharmaceutical therapy applications, the use of alpha-emitting radionuclides is growing in popularity for treatment of cancer due to their high energy deposition and potential for localized targeting. The design of intravenously administered therapies leveraging the short-range of alpha particles (50-100 µm) requires accurate dosimetry calculations. Current computational models used for these calculations, however, do not include tissue level details that incorporate the spatial patterns associated with blood microvessels, lymphatic vessels, or other anatomically relevant details.

The objective of this study was to develop a set of 3D computational, tissue-representative models incorporating physiologically relevant microvascular network patterns for calculating local alpha-particle and electron dosimetry effects.

## MATERIALS AND METHODS

Adult rat mesenteric tissues labeled for PECAM and Lyve-1 were imaged. Images were imported into Creo Parametric and converted to a 3D polygon mesh model, then a tetrahedral mesh using POLY2TET. The model was then incorporated into PHITS and absorbed fractions were computed for the blood microvascular, lymphatic and interstitial regions. Simulations were performed for alpha particles of energies 1-12 MeV in increments of 0.5 MeV and for electrons on a logarithmic energy grid from 10 keV to 10 MeV.

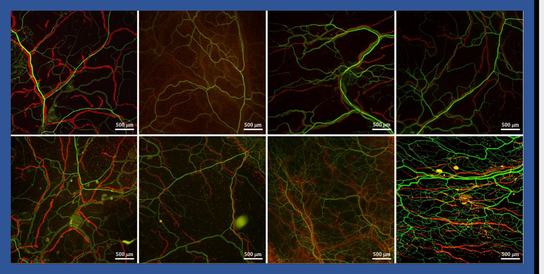

**Figure 1. Imaged regions of interest.** Eight regions of interest included and modeled of blood vasculature (green) and lymphatic vasculature (red) – regions 1-4 (top row, left to right) and regions 5-8 (bottom row, left to right). Regions 7 and 8 are angiogenically stimulated, while 1-6 are unstimulated.

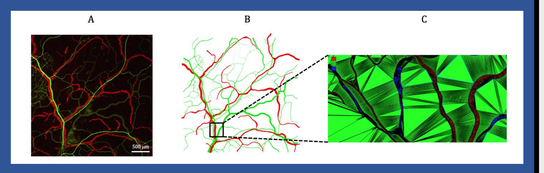


**Figure 2. Model construction overview.** (A) Image of a selected ROI in an unstimulated rat mesenteric microvascular network. Vessels were identified via labeling with PECAM (green) for blood vasculature and Lyve-1 (red) for lymphatic vasculature, (B) 3D polygon mesh model with blood (green) and lymphatics (red) modeled, and (C) 3D tetrahedral mesh model with blood (red), lymphatics (blue) and interstitial tissue (green).

## RESULTS

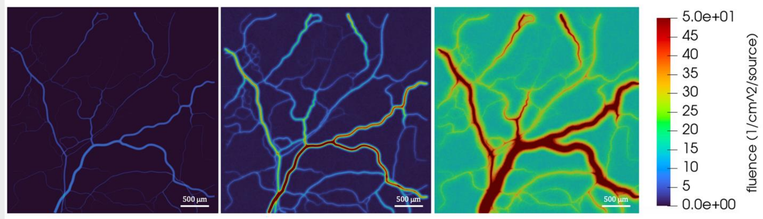


**Figure 3. Particle fluence heat maps.** Particle fluence across the ROI with the radiation source starting in the blood, where red represents highest particle fluence, and navy represents the lowest, from source particles of increasing energy from left to right – 1 MeV (left), 6 MeV (middle) and 12 MeV (right) alpha particles.

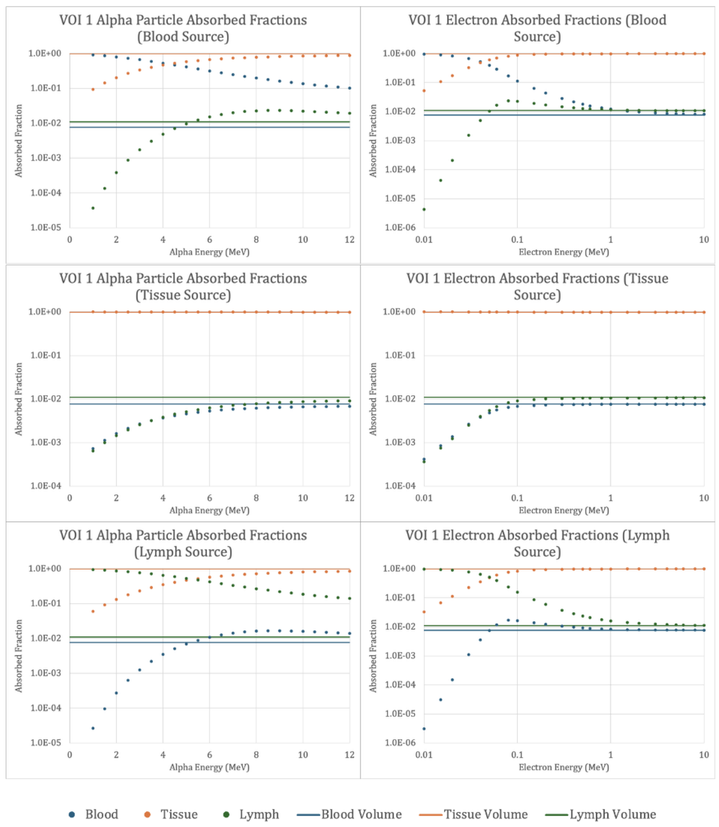


**Figure 4. Absorbed fractions in VOI 1.** Energy absorbed in blood, lymph, and tissue from a blood source (top), tissue source (middle), and lymphatic source (bottom) across alpha particle energies up to 12 MeV (right column) and electron energies up to 10 MeV (left column), along with the relative volume fractions of each region.

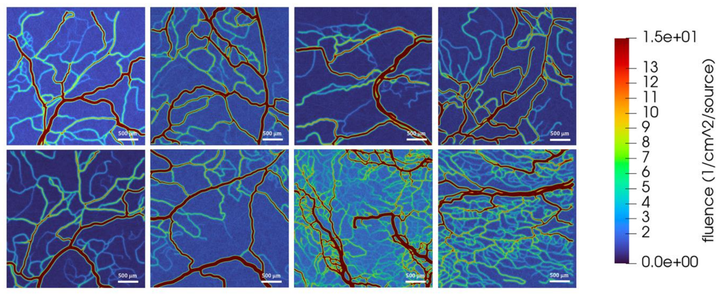


**Figure 5. Heat Maps of Fluence at Constant Energy in All Different VOIs.** The comparison of particle fluence of a constant energy (6 MeV alpha particles) from a blood vessel source across different VOIs in order to visualize the effect of vessel size, layout, and density on the distribution.

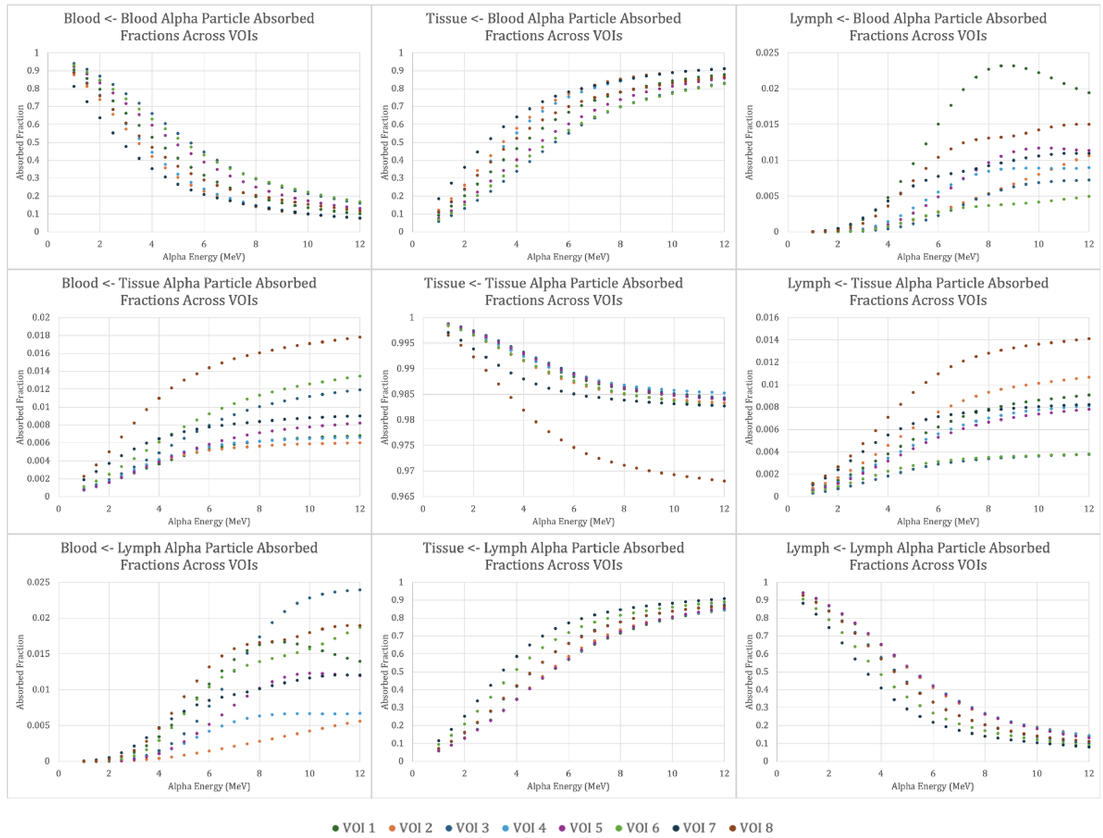


**Figure 6. Alpha Particle Absorbed Fractions in All Different VOIs.** Absorbed fractions across all sources and targets in all VOIs for alpha particles.

**Table 1. Volume Fractions of VOIs.** Volumes of blood, lymphatics, and soft tissue in each VOI, as well as relative fractions of each.

| VOI Number | Blood Volume ($cm^3$) | Lymphatic Volume ($cm^3$) | Soft Tissue Volume ($cm^3$) | Total Volume ($cm^3$) | Blood Volume Fraction (%) | Lymphatic Volume Fraction (%) | Soft Tissue Volume Fraction (%) |
|---|---|---|---|---|---|---|---|
| 1 | 1.57e-5 | 2.24e-5 | 2.01e-3 | 2.05e-3 | 0.764 | 1.090 | 98.146 |
| 2 | 1.03e-5 | 2.01e-5 | 1.53e-3 | 1.56e-3 | 0.658 | 1.289 | 98.053 |
| 3 | 3.79e-5 | 1.16e-5 | 2.64e-3 | 2.69e-3 | 1.410 | 0.433 | 98.157 |
| 4 | 1.50e-5 | 2.04e-5 | 2.05e-3 | 2.09e-3 | 0.721 | 0.979 | 98.300 |
| 5 | 2.45e-5 | 2.39e-5 | 2.57e-3 | 2.62e-3 | 0.936 | 0.913 | 98.151 |
| 6 | 2.42e-5 | 6.57e-6 | 1.47e-3 | 1.50e-3 | 1.614 | 0.438 | 97.948 |
| 7 | 1.07e-5 | 1.01e-5 | 1.05e-3 | 1.07e-3 | 1.000 | 0.937 | 98.063 |
| 8 | 3.04e-5 | 2.47e-5 | 1.45e-3 | 1.51e-3 | 2.021 | 1.638 | 96.341 |

## CONCLUSIONS

Our results provide the first estimates of alpha and electron absorbed fractions associated with experimentally derived blood and lymphatic microvascular structures and serve to guide whether such tissue level detail should be considered in pre-clinical treatment planning. An appreciation of the influence of microvessel size, patterning, and density on absorbed fractions provides a valuable perspective on the importance of the consideration of microvessels in models used in radiation applications in the field – suggesting the increasing utility of patient-specific, detailed models for optimization of personalized dosimetry. The results motivate future studies that incorporate other rat tissues imaged at depth, expansion into analogous algorithmically generated microvascular capillary networks, and generalization to human capillary network models.

UF UNIVERSITY of FLORIDA
J. Crayton Pruitt Family Department of Biomedical Engineering

## CONTACT & FUNDING INFORMATION

Julia Withrow, juliawithrow@ufl.edu

NIH R01 CA248901, NIH Fellowship F31 HL182303, and NSF 2309559

ALRADS

© Poster Template by Genigraphics® 1.800.790.4001 www.genigraphics.com